J. Comput. Appl. Res. Mech. Eng. Vol. 10. No. 2, pp. 511-524, 2021 *DOI: 10.22061/jcarme.2019.5265.1653*

SRTTU

Journal of Computational and Applied Research in Mechanical Engineering

jcarme.sru.ac.ir

JCARME

ISSN: 2228-7922

Research paper

Investigation of temperature jump and slip effects on nanofluid treatment inside a vertical annulus via modified Buongiorno's model

Hamid Reza Ghaffarianjam[a,*], Sajad A. Moshizi[b], Mahdi Zamani[c] and Mahdi Amiri Daluee [d]

[a]*Islamic Azad University, Gonabad Branch, Department of Mechanical Engineering, Gonabad, Iran*
[b]*Young Researchers and Elite Club, Neyshabur Branch, Islamic Azad University, Neyshabur, Iran*
[c]*Department of Mechanical Engineering, Ferdowsi University of Mashhad, Mashhad, Iran*
[d]*Faculty of Civil Engineering and Environment, Khavaran Institute of Higher Education, Mashhad, Iran*

Article info:

Article history:

Received: 15/05/2019
Accepted: 11/12/2019
Revised: 14/12/2019
Online: 16/12/2019

Keywords:

Nanofluid,
Modified Buongiorno's model,
Temperature jump,
Slip velocity,
Mixed convection.

[*]Corresponding author:
ghaffarian_jam@yahoo.com

Abstract

In the present work, the study of alumina-water nanofluid heat transfer between two concentric vertical cylinders has been done by modified Buongiorno's model (BM) to examine the impacts of temperature jump and slip velocity boundary conditions for a wide range of Knudsen number. Runge-Kutta-Fehlberg method, as a standard integration scheme along with a shooting method, has been chosen for solving nonlinear ordinary differential equations (ODEs) along with boundary conditions. The main concentration of this paper is on the temperature jump since the slip velocity has been extensively examined in many studies. The presence of temperature jump boundary condition by varying Knudsen number was considered to investigate the effects of the bulk mean nanoparticle volume fraction ϕ_B, mixed convection parameter *Nr*, buoyancy parameter *Ng*, and heat flux ratio ε on the total dimensionless heat transfer coefficient *HTC* and the dimensionless pressure gradient N_{dp}. The obtained results indicate that temperature jump boundary condition plays a pivotal role in temperature profile, heat transfer coefficient and pressure drop; for instance, the negligence of temperature jump near walls causes to undervalue heat transfer coefficient in continuum flow regime and overestimate it in slip flow regime.

1. Introduction

Incorporation of particles into the prevalent fluids like water, oil and ethylene-glycol as one of the ways of passive heat transfer enhancement was pioneered in 1873 by Maxwell [1]. The solid particles must possess a higher thermal conductivity, thereby enhancing the thermal conductivity of generated mixture (solid-fluid). After investigating the impact of particles inclusion to fluids on the possible improvement of heat transfer, many researchers concluded that adding nanoparticles to a base fluid outperforms micro-sized particles on the grounds of mitigating the deleterious effects of clogging, abrasion, fouling and extra pressure loss [2, 3].

Thus, using nanofluids to enhance the heat transfer rate is fast gaining popularity among researchers, and comes into widespread use in the heat transfer systems and exchangers.

Nanofluid convective simulation was studied by several researchers in a wide range of diverse topics. Heat transfer analysis of fluids with the addition of nanoparticles is currently attracting considerable interests. The importance of adding nanoparticles to the base fluid is owing to the significant heat transfer augmentation with the presence of nanofluids. Therefore, this heat transfer in nanofluids has been studied with considerations of various aspects such as magnetic field [4-11], porous medium [4, 12] and entropy generation and exergy loss [13, 14]. Recently, Kerdarian and Kianpour [15] used the finite volume method and SIMPLER algorithm to study entropy generation and heat transfer in a microchannel filled with Cu-water nanofluid. They studied a broad range of Reynolds numbers, Knudsen numbers and nanoparticles volume fraction.

Theoretical modelling of nanofluids receives wide currency among scientists due to clarifying the thermophysical characteristics of nanofluids. From the literature review, the critical mechanism significantly influencing the heat transfer and flow features of nanofluids is the nanoparticle migration. Buongiorno [16] proved that seven mechanisms result in the nanoparticle migration, among which the thermophoresis and Brownian motion are the most important mechanisms. These two factors generate a relative velocity due to the interaction of the base fluid and nanoparticles. Accordingly, Buongiorno presented a two-component four-equation non-homogeneous equilibrium model for scrutinising the convective transport in nanofluids. In the light of the BM, many researchers such as Sheikholeslam [17], Moshizi and Pop [18],Grosan and Pop [19], Aziz et al. [20], Bahiraei et al. [21], Moshizi et al. [22-24] and Xu et al. [25] have studied nanofluids by considering heat transfer. Afterwards, the modified version of the BM including the nanofluid density (ρ) variation in continuity, momentum and energy equations was developed by Yang et al. [26, 27]. This modification thoroughly deems the impacts of nanoparticle concentration on the governing equations. Using the modified BM, they investigated the fully developed forced convection in nanofluids inside an annulus. Then, several studies were done on different heat transfer features including natural [28] forced [29, 30], and mixed convection [31] via the modified model. The results revealed that the effects of nanoparticle migration in nanofluids are well captured by the modified model.

However, the studies mentioned above were restricted to special boundary conditions at walls such as non-jump temperature and non-slip velocity. While these boundary conditions are not capable of estimating the precise velocity and temperature profiles for some of the microscope applications [32, 33]. Smoluchowski [34] and Knudsen [35] pioneer the temperature jump as a classic physical phenomenon. According to Knudsen number $Kn = \lambda / L$ in which λ and L are the molecular mean free path and physical scale of flow domain respectively, fluid flow is categorized as these flow regimes, namely:

Continumflow	$Kn \leq 0.001,$
Slipflow	$0.001 < Kn \leq 0.1,$
Transitionflow	$0.1 < Kn \leq 10,$
Freemolecularflow	$10 < Kn.$

In fact, no-jump/no-slip conditions are suitable for the fluid flow with the thermodynamic equilibrium in the vicinity of the walls where this situation occurs in the continuum flow regime (as long as $Kn < 0.001$) [36]. This range of Kn is indicative of macro-scale devices, while Kn in the range between 0.001 and 0.1, and $Kn \approx 0.1$ represent micro-scale and nano-scale means respectively. In the micro- and nano-scale devices, temperature jump and slip velocity at walls are required [37-39]. Taking advantage of nanofluids as working fluids can be considered as another innovative approach to improve the convective heat transfer rate in the micro and nano-scale devices. Karimipour [40] studied the impact of temperature jump and slip velocity on the heat transfer of several nanofluids in a microchannel. Yang et al. [37] used the modified BM to probe the impacts of temperature jump and slip velocity near walls for different flow

regions. They investigated the forced convection transport of nanofluids in a straight channel and concluded that applying temperature jump close to walls is so necessary, especially in slip flow regime. Recently, Sajadifar et al. [41] investigated a non-Newtonian nanofluid inside a microtube in light of temperature jump and slip velocity at walls. They concluded that the temperature jump effects should be considered at the microtube entrance area where the most heat exchange with the wall happened.

The novelty of this work is to examine the impacts of the temperature jump and slip velocity in continuum and slip flow regimes on the mixed convection of Al-water nanofluid with focus on the influence of temperature jump on the velocity, temperature, volume fraction of nanoparticles, heat transfer coefficient, and pressure drop.

2. Problem definition

In this study, the two-dimensional, hydrodynamically fully developed, laminar mixed convection flow of Al-water nanofluid in a vertical annulus subject to unequal heat flux on the interior and exterior walls are investigated. The vertical annulus is made of two coaxial cylinders with the Cartesian coordinate in which x-direction runs along the pipe walls, the r-direction is perpendicular to them, and the origin of the coordinate system is located at the interior wall, as shown in Fig. 1. q''_{wi} and q''_{wo} are heat fluxes uniformly subject to the inner and outer walls respectively in such a way that the heat flux ratio, ε, varies between 0 and 1. This parameter is an indicator of the thermal asymmetry. Owing to micro- and nano-scale flow domain ($0.001 < Kn \leq 0.1$), temperature jump and slip velocity are two pivotal parameters as boundary conditions, which must be considered in the slip flow regime [37, 42]. Furthermore, nanoparticles influence the heat and mass transfer as the properties of the nanofluid are a function of nanoparticles volume fraction of the nanofluid obtained via [43]

$$\rho = \phi\rho_p + (1-\phi)\rho_{bf}, \quad (1)$$

$$\mu = \mu_{bf}\left(1 + a_\mu\phi + b_\mu\phi^2\right), \quad (2)$$

$$k = k_{bf}\left(1 + a_k\phi + b_k\phi^2\right), \quad (3)$$

$$c_p = \frac{\phi\rho_p c_{p_p} + (1-\phi)\rho_{bf} c_{p_{bf}}}{\phi\rho_p + (1-\phi)\rho_{bf}}, \quad (4)$$

where ρ, μ, k, and c_P are the density, dynamic viscosity, thermal conductivity, and specific heat capacity of nanofluid, respectively; and the subscripts of p and bf signify nanoparticle and base fluid. The thermophysical properties of nanoparticles and base fluid (water) are outlined in Table 1. Eqs. (2 and 3) represent thermal conductivity and viscosity of nanofluids estimated by Pak and Cho [44] respectively.

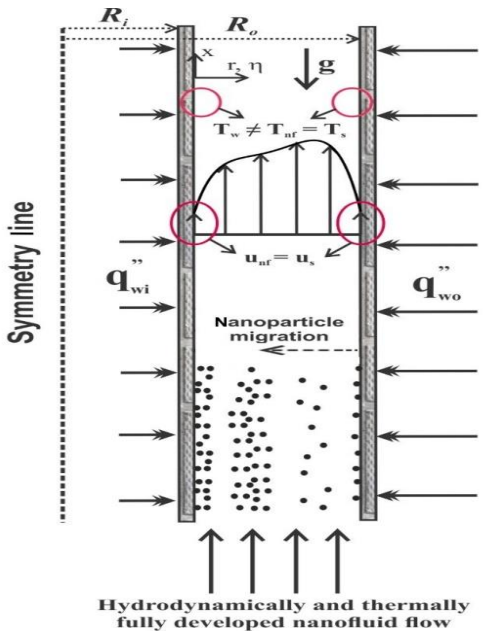

Fig. 1. Schematic diagram of the physical problem and coordinate system.

Table 1. Thermophysical properties of the base fluid and the nanoparticles.

Physical properties	Fluid phase (water)	Alumina (Al_2O_3)
c_p (J kg^{-1} K^{-1})	4182	773
ρ (kg m^{-3})	998.2	3880
k (W m^{-1} K^{-1})	0.597	36
$\mu\times10^4$ (kg m^{-1} s^{-1})	9.93	-
β (K^{-1})	2.07×10^{-4}	8.4×10^{-6}

3. Formulation of the problem

The mathematical formulation of nanofluid flow proposed by Buongiorno [16] is widely employed to simulate the hydrodynamically and thermally fully developed flow inside the vertical annulus.
In the BM, the variation of nanofluid properties such as density, dynamic viscosity and thermal conductivity originating from the non-uniform concentration of nanoparticles was not considered. Therefore, the modified BM proposed by Yang et al. [27] is used to incorporate the effect of nanoparticle distribution on thermophysical properties of nanofluid into the equations of the mass, momentum, thermal energy, and nanoparticle fraction:

$$\frac{1}{r}\frac{d}{dr}\left(r\mu(\phi)\frac{du}{dr}\right)-\frac{dp}{dx} -\left(\rho_p-\rho_{bf_0}\right)\left(\phi-\phi_{wo}\right)g +\left(1-\phi_{wo}\right)\rho_{bf_0}\beta\left(T-T_B\right)g=0 \quad (5)$$

$$\rho(\phi)c(\phi)u\frac{dT}{dx}= \frac{1}{r}\frac{d}{dr}\left(rk(\phi)\frac{dT}{dr}\right) \quad (6)$$

$$\frac{1}{r}\frac{\partial}{\partial r}\left(D_B\frac{\partial\phi}{\partial r}+\frac{D_T}{T}\frac{\partial T}{\partial r}\right)=0 \quad (7)$$

Where u, T and P represent the axial velocity, local temperature and pressure, respectively. Also, $D_B=\left(k_{BO}T\right)/\left(3\pi\mu_{bf}d_p\right)$ is the Brownian diffusion coefficient and thermophoretic diffusion coefficient are defined as $D_T=\phi\left(0.26k_{bf}\mu_{bf}\right)/\left[\left(2k_{bf}+k_P\right)\rho_{bf}\right]$ in which k_{BO} is the Boltzmann constant and d_p is the nanoparticle diameter which varies between 1 and 10 nm [44].
Considering Eqs. (5-7), it is worth noting that the modified BM consists of the density variation of nanofluid in mass, momentum and energy conservations. Since ρ is highly dependent on ϕ, the modified BM deems the impacts of nanoparticle diffusion, as seen in Eqs. (1-4).

The function of averaging any required variables over the annulus cross-section should be defined by

$$\bar{\varphi}\equiv\frac{1}{A}\int_A\varphi dA= \frac{1}{\pi\left(R_o^2-R_i^2\right)}\int_{R_i}^{R_o}2\pi r\varphi dr \quad (8)$$

So, with averaging the energy equation (Eq. (6)), a bulk temperature gradient is obtained as below

$$\overline{\rho(\phi)c(\phi)u}\frac{dT_B}{dx}= \frac{4q''_{wo}}{D_h\left(1+\frac{R_i}{R_o}\right)}\left(1+\frac{R_i}{R_o}\frac{q''_{wi}}{q''_{wo}}\right) \quad (9)$$

in which the bulk temperature is defined as

$$T_B\equiv\frac{\overline{\rho cuT}}{\overline{\rho cu}}. \quad (10)$$

Also, note that under thermally fully developed flow condition with a constant heat flux at walls, across the x-axis, the temperature gradient is not dependent on cross-section temperature and can be defined as

$$\frac{\partial T}{\partial x}=\frac{\partial T_B}{\partial x} \quad (11)$$

4. Boundary conditions

In this study, since continuum and slip flow regimes are examined, walls experience the slip and jump conditions. The first-order slip at both walls is expressed as [45]

$$r=R_{wi}\ \rightarrow\ u_s-u_w=\frac{2-\sigma_v}{\sigma_v}\lambda\frac{\partial u}{\partial r}$$
$$r=R_{wo}\ \rightarrow\ u_s-u_w=-\frac{2-\sigma_v}{\sigma_v}\lambda\frac{\partial u}{\partial r} \quad (12)$$

where u_s is the slip velocity, σ_v is the tangential momentum accommodation coefficient, and λ is the molecular mean free path. The temperature jump at either wall is defined as [45]

$$r = R_{wi} \rightarrow T_s - T_w = \frac{2-\sigma_T}{\sigma_T}\frac{2\beta}{\beta+1}\frac{\lambda}{\Pr}\frac{\partial T}{\partial r}$$
$$r = R_{wo} \rightarrow T_s - T_w = -\frac{2-\sigma_T}{\sigma_T}\frac{2\beta}{\beta+1}\frac{\lambda}{\Pr}\frac{\partial T}{\partial r} \quad (13)$$

Where T_w is the wall temperature, while T_s is the temperature of nanofluid at the wall. σ_T is the thermal accommodation coefficient, and β is the specific heat ratio. σ_v, σ_T and β are considered to be close to one for nearly all applications [37, 45]. Therefore, these parameters are opted to be one for simplicity in this study.
The other existing boundary conditions are stated as follows

$$\begin{aligned} &r = R_{wi} \text{ (on the inner wall)} \rightarrow \\ &-k_{wi}\frac{\partial T}{\partial r} = q''_{wi}, \\ &D_B\frac{\partial \phi}{\partial r} + \frac{D_T}{T}\frac{\partial T}{\partial r} = 0 \\ &r = R_{wo} \text{ (on the outer wall)} \rightarrow \\ &k_{wo}\frac{\partial T}{\partial r} = q''_{wo}, \\ &D_B\frac{\partial \phi}{\partial r} + \frac{D_T}{T}\frac{\partial T}{\partial r} = 0 \end{aligned} \quad (14)$$

5. Normalization

In order to more accurately evaluate the physical problem and reach a linear and more robust relationship, the governing equations are normalized, so the dimensionless parameters are defined as follows

$$\begin{aligned} &\eta = \frac{2r}{D_h}, u^* = \frac{u}{\frac{D_h^2}{\mu_{bf}}\left(-\frac{dp}{dx}\right)}, \\ &\theta = \frac{T - T_{so}}{\frac{\left(q''_{wo} + q''_{wi}\right)D_h}{k_{bf}}}, \\ &\zeta = \frac{R_{wi}}{R_{wo}},\ \varepsilon = \frac{q''_{wi}}{q''_{wo}}, Nr = \frac{\left(\rho_p - \rho_{bf_0}\right)g}{\left(-dp/dx\right)}, \\ &Ng = \frac{\rho_{bf_0}\beta g q''_{wo} D_h}{\left(-dp/dx\right)k_{bf}}, \gamma = \frac{\left(q''_{wo} + q''_{wi}\right)D_h}{T_B k_{bf}}, \\ &N_{BT} = \frac{D_{B_B} k_{bf} T_B \phi_B}{D_{T_B} D_h \left(q''_{wo} + q''_{wi}\right)} \end{aligned} \quad (15)$$

Therefore, based on these dimensionless parameters, the normalized governing equations are obtained as below

$$\begin{aligned} \frac{d^2u^*}{d\eta^2} = &-\left(\frac{1}{\eta} + \frac{1}{\mu(\phi)}\frac{d\mu(\phi)}{d\phi}\frac{d\phi}{d\eta}\right)\frac{du^*}{d\eta} \\ &-\frac{\mu_{bf}}{4\mu(\phi)}\left[1 - Nr\left(\phi - \phi_{wo}\right) + Ng\left(1-\phi_{wo}\right)\left(\theta^* - \theta_B^*\right)\right] \end{aligned} \quad (16)$$

$$\begin{aligned} \frac{d^2\theta}{d\eta^2} = &-\frac{k_{bf}}{k(\phi)} \\ &\left[-\frac{\rho(\phi)c_p(\phi)u^*}{\rho(\phi)c_p(\phi)u^*}\left(\frac{(1+\zeta\varepsilon)}{(1+\zeta)(1+\varepsilon)}\right) + \left(7.47\frac{d\phi}{d\eta} + \frac{k(\phi)/k_{bf}}{\eta}\right)\frac{d\theta}{d\eta}\right] \end{aligned} \quad (17)$$

$$\frac{\partial \phi}{\partial \eta} = -\frac{\phi}{N_{BT}\left[1 + \gamma\left(\theta^* - \theta_B^*\right)\right]^2}\frac{\partial \theta}{\partial \eta} \quad (18)$$

Since the presented equations are in terms of T_{so}, using Eq. (13) and the following correlation

$$T - T_{wo} = \left(T - T_{so}\right) - \left(T_{wo} - T_{so}\right), \quad (19)$$

θ can be transformed into Eq. (20) as follows

$$\begin{aligned} &\theta^* = \frac{T - T_{wo}}{\frac{\left(q''_{wo} + q''_{wi}\right)D_h}{k_{bf}}} = \\ &\theta - \frac{2Kn}{\Pr}\frac{\partial \theta}{\partial \eta}\Big|_{\eta = \frac{1}{1-\zeta}} \end{aligned} \quad (20)$$

Accordingly, the bulk temperature given in Eq. (16 and 18) yields as below

$$\theta_B^* = \frac{T_B - T_{wo}}{\frac{\left(q''_{wo} + q''_{wi}\right)D_h}{k_{bf}}}. \quad (21)$$

Also, dimensionless boundary conditions can be determined as

$$\eta=\frac{\zeta}{1-\zeta}\ (\text{inner wall})\rightarrow$$
$$\frac{d\theta}{d\eta}=-\frac{\varepsilon}{2(1+\varepsilon)}\frac{k_{bf}}{k_{wi}},$$
$$u^*=u_s^*=2Kn\left.\frac{du^*}{d\eta}\right|_{\eta=\frac{\zeta}{1-\zeta}}$$
$$\eta=\frac{1}{1-\zeta}\ (\text{outer wall})\rightarrow \tag{22}$$
$$\theta=0,\ \frac{d\theta}{d\eta}=\frac{1}{2(1+\varepsilon)}\frac{k_{bf}}{k_{wo}},$$
$$u^*=u_s^*=-2Kn\left.\frac{du^*}{d\eta}\right|_{\eta=\frac{\zeta}{1-\zeta}},\ \phi=\phi_{wo}$$

where $Kn=\lambda/D_h$ is Knudsen number and ε presents the heat flux ratio. Based on the dimensionless parameters, Eq. (9), the dimensionless bulk temperature gradient is presented as

$$\overline{\rho(\phi)c(\phi)u^*}\frac{dT_B}{dx}=\frac{4q_{wo}''}{D_h}\frac{(1+\zeta\varepsilon)}{(1+\zeta)} \tag{23}$$

where the dimensionless function of averaging any required parameters is defined as

$$\bar{\varphi}=\frac{2(1-\zeta)^2}{(1-\zeta^2)}\int_{\frac{\zeta}{1-\zeta}}^{\frac{1}{1-\zeta}}\eta\varphi d\eta \tag{24}$$

Moreover, the dimensionless heat transfer coefficients are defined for the inner wall

$$HTC_{wi}=\frac{h_iD_h}{k_{bf}}=\frac{q_{wi}''D_h}{k_{bf}(T_{wi}-T_B)}$$
$$=\frac{\varepsilon}{(\theta_{wi}^*-\theta_B^*)(1+\varepsilon)}, \tag{25}$$

and for outer wall

$$HTC_{wo}=\frac{h_{wo}D_h}{k_{bf}}=\frac{q_{wo}''D_h}{k_{bf}(T_{wo}-T_B)}$$
$$=-\frac{1}{\theta_B^*(1+\varepsilon)}. \tag{26}$$

So the total *HTC* is calculated for the annulus as

$$HTC=\frac{R_iHTC_{wi}+R_oHTC_{wo}}{R_i+R_o}$$
$$=\frac{\zeta HTC_{wi}+HTC_{wo}}{\zeta+1}. \tag{27}$$

Therefore, the total heat transfer coefficient enhancement is obtained as

$$N_h=\frac{HTC}{HTC_{bf}}. \tag{28}$$

Similarly, the dimensionless pressure gradient is evaluated as

$$N_{dp}=\left(-\frac{dp}{dx}\right)\Big/\left(\frac{\mu_{bf}u_B}{D_h^2}\right)=\frac{\rho_B}{\overline{\rho u^*}} \tag{29}$$

As a result, the N_{dp} augmentation is defined as

$$N_p=\frac{N_{dp}}{(N_{dp})_{bf}} \tag{30}$$

6. Numerical method and accuracy

The aforementioned equations, Eqs. (16, 17 and 18) present a set of nonlinear ordinary differential equations (ODEs) along with the boundary conditions of Eq. (22). The suitable and accurate approach chosen for solving this system is the Runge-Kutta-Fehlberg method as a standard integration scheme [46-48]. This method presents the numerical solution with the order $O(h^4)$ and estimates errors with the order of $O(h^5)$. But, ϕ_{wo} in the boundary condition, and $\overline{\rho(\phi)c(\phi)u^*}$ in Eq. (17) are initially unknown, so a reciprocal procedure is requisite for solving the system of equations with initial guesses for these unknown parameters. The checking points for

updating these parameters are the bulk nanoparticle volume fraction ϕ_B and $\overline{\rho(\phi)c(\phi)u^*}$ which are calculated and finally compared with the presumed value of $\overline{\rho(\phi)c(\phi)u^*}$ and the specified value of ϕ_B. Therefore, this procedure must be iterated so that the specified value of ϕ_B is gained, and the exact value of $\overline{\rho(\phi)c(\phi)u^*}$ is achieved with a relative error less than 1%. This method is a kind of shooting technique. In order to keep away from the grid dependency, the integration step was varied around 10^{-6}.

In order to corroborate the high accuracy of different parts of the numerical analyse, the velocity profile is compared to the data of Kays et al. [49] in Fig. 2. On the other hand, the thermal boundary condition is validated with the dimensionless heat transfer coefficients at both walls with the study of Kays and Crawford [50] presented in Table 2. As is observed, the main features of this problem (velocity and heat transfer) have been compared with the data available in the literature. The obtained results indicate that different methods for modelling this problem reach the same results with a relative difference less than 1%. Furthermore, in order to ensure the validation of the developed code and the applied methods, the velocity profile within the concentric annulus is calculated by the present work and compared with the results of Yang et al [26], as illustrated in Fig. 3.

7. Results and discussion

The objective of this part is to scrutinize the impacts of Knudsen number *Kn* and temperature jump on velocity profile, temperature and nanoparticle volume fraction distributions, along with the effects of ϕ_B, mixed convection parameter *Nr*, buoyancy parameter *Ng*, and heat flux ratio ε on *HTC* and N_{dp} in the range of Knudsen numbers. The predetermined parameters are deemed to be $\varepsilon = 1.0$, $Kn = 0.05$, $N_{BT} = 0.2$, $\phi_B = 0.02$, $Nr = 200$, $Ng = 10$, and $\Pr = 7.0$. The results have been done for various values of influential parameters. According to Yang et al. [26], $\gamma \cong \frac{T_w - T_B}{T_w}$ insignificantly influences the results, and ranges from 0 to 0.1, so γ has a prescribed value in this study, $\gamma = 0.01$. Furthermore, $\eta = 1$ represents the inner wall, whereas the outer wall is located in $\eta = 2$.

Table 2. Numerical results for HTC with the ones presented in the previous work when $Nr=\lambda=\phi_B=Ha=0$.

ζ	ε	Present work		Kays and Crawford [50]	
		HTC_{wi}	HTC_{wo}	HTC_{wi}	HTC_{wo}
0.2	1.5	21.42	5.785	21.42	5.787
	1	89.46	5.465	89.46	5.450
	0.5	-10.54	5.149	-10.49	5.151
	0	0	4.875	0	4.883
0.6	1.5	8.68	8.075	8.63	8.071
	1	11.21	6.749	11.21	6.758
	0.5	109.4	5.810	109.48	5.812
	0	0	5.091	0	5.099

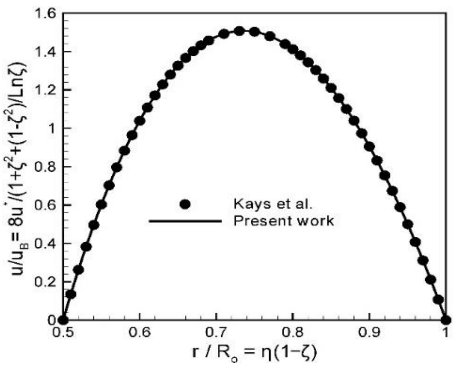

Fig. 2. Velocity profile within the concentric annulus calculated by the present work and the data of Kays et al. [49].

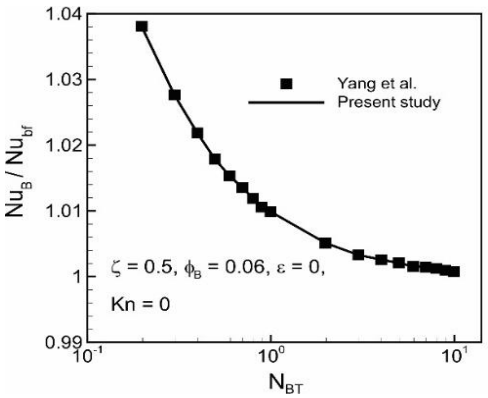

Fig. 3. Velocity profile within the concentric annulus calculated by the present work and the data of Yang et al. [26].

Figs. 4(a-c) reveal the effects of Knudsen number variation on the velocity, temperature profiles and nanoparticle volume fraction distribution. As is evident from Fig. 4(a), increasing *Kn* causes the velocity near walls to rise, on the grounds that the slip velocity grows in the boundaries. Consequently, the velocity of nanofluids speeds up close to walls and owing to a constant mass flux in the annulus, and the velocity becomes lower in the middle. So the velocity of nanofluids gets more uniform as Knudsen number (*Kn*) rises, as supported in Fig. 4(a). It results in the momentum amplification at walls, thereby increasing the temperature and concentration of nanoparticles inside the annulus. On the other side, the increase in *Kn* leads to extend the influence of the temperature jump and slip velocity on the temperature profile. Both these boundary conditions are influential parameters on the temperature close to walls, as shown in Fig. 4(b). By increasing the temperature and velocity at walls, the nanoparticles concentration in these regions rises as indicated in Fig. 4(c).

Figs. 5(a-c) illustrate how the existence of the temperature jump at boundaries influences the velocity, temperature profiles, and nanoparticle volume fraction distribution. According to Figs. 5(a and c), the results indicate that the effect of the temperature jump on the velocity profile and nanoparticle volume fraction distribution for the high and low values of *Kn* is trivial as supported by the results of Yang et al. [37]. However, considering the temperature jump at walls leads to significantly change the temperature profile due to the boundary condition defined in Eq. (13). It is demonstrated that in the high values of *Kn*, the temperature profile tends to be uniform with increasing the temperature at walls and decreasing the peak in the case of considering the temperature jump, while in low values of *Kn*, there are subtle differences between both cases with and without temperature jump as shown in Fig. 5(b).

Figs. 6-9 delineate the behaviour of *HTC* and N_{dp} under the variation of ϕ_B, *Nr*, *Ng*, and ε, respectively. All results are calculated based on a wide range of *Kn* indicative of the continuum flow and slip flow regimes. It is worthwhile to note that irrespective of the variation of the aforementioned parameters, the pressure drop experiences a downward trend in the case of applying the temperature jump under the variation of *Kn*. This decreased rate significantly grows from *Kn*=0.01 in the slip flow regime. From Fig. 6, it is clear that regardless of the value of *Kn* and the existence of the temperature jump, an increase in ϕ_B enhances the heat transfer rate with the penalty of pertaining pressure drop increase. Moreover, in the slip flow regime, the temperature jump at walls curtails the heat transfer rate and also the pressure drop compared to the case without consideration of temperature jump; however, this behaviour is reversed in the continuum flow regime for all the values of ϕ_B except for $\phi_B = 0.01$. In the high value of ϕ_B, the difference in *HTC* between both cases of the temperature jump rises.

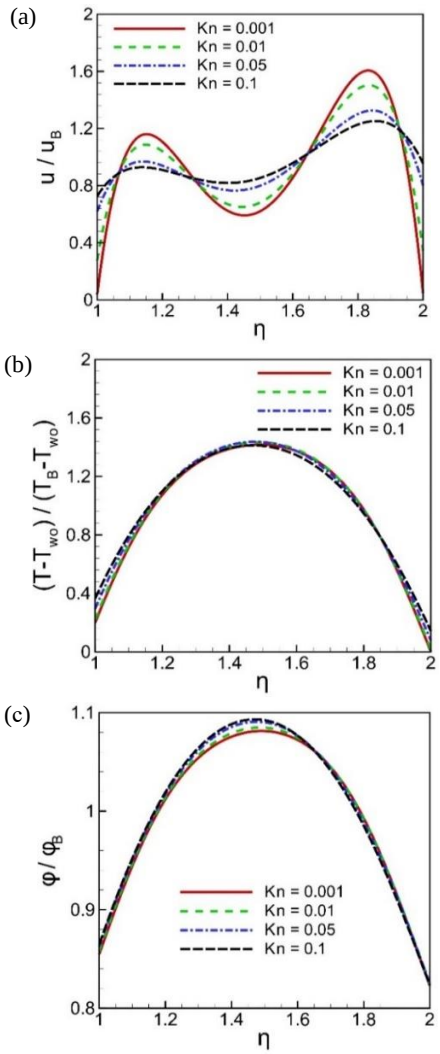

Fig. 4. Effect of *Kn* on velocity profile (a), temperature (b), nanoparticle volume fraction distributions (c).

Fig. 7 reveals the variation of *HTC* and N_{dp} in terms of different mixed convection parameters, *Nr* in two flow regimes with and without temperature jump conditions. Basically, *Nr* signifies the intensity of buoyancy effect owing to nanoparticle concentration and base on the definition, *Nr* influences nanofluids to transport nanoparticles from the rich concentration region towards the poor concentration one. The most crucial point is that *Nr* is a buoyancy diffusion caused by uneven nanoparticles concentration. So, *Nr* considerably intensifies heat transfer and pressure drop.

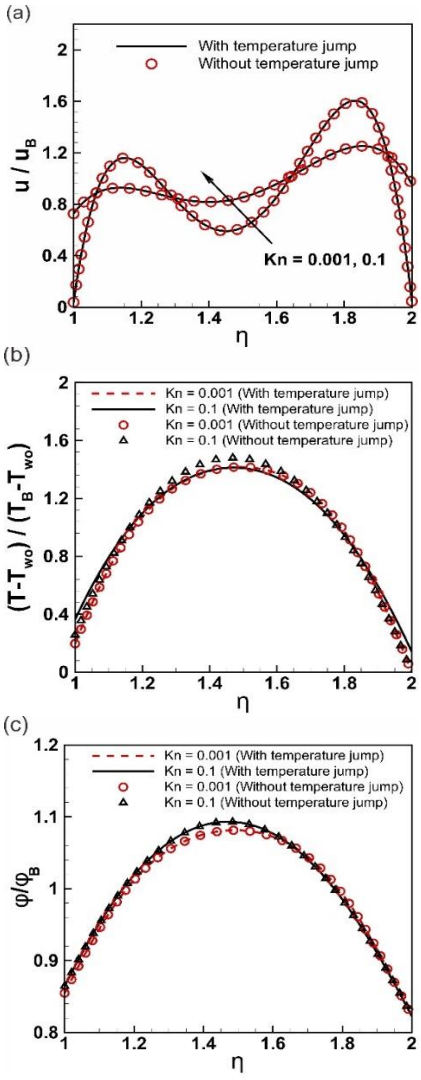

Fig. 5. Effect of temperature jump on velocity profile (a), temperature (b), nanoparticle volume fraction distributions (c) (symbol sign: without temperature jump, and line curve: with temperature jump).

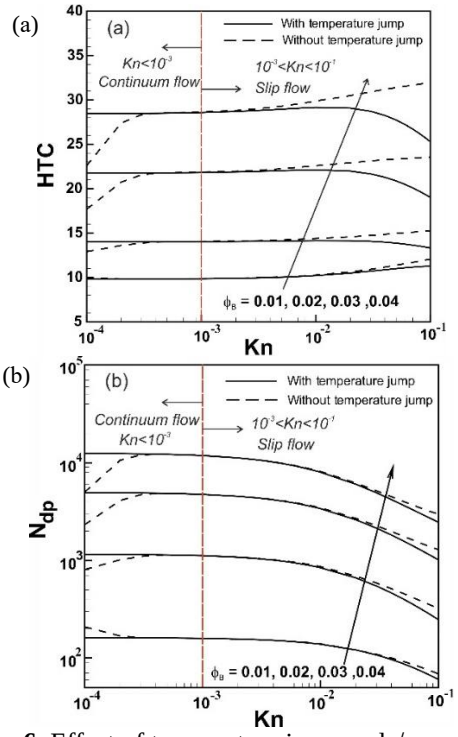

Fig. 6. Effect of temperature jump and ϕ_B on *HTC* (a) and N_{dp} (b) (dash line: without temperature jump, and solid line: with temperature jump)

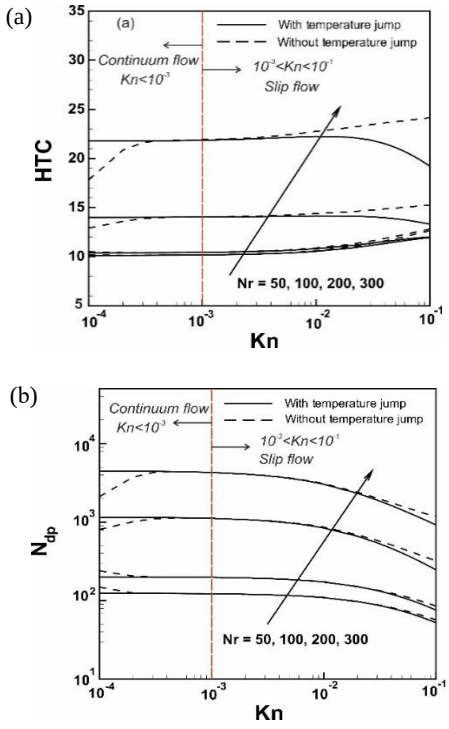

Fig. 7. Effect of temperature jump and *Nr* on *HTC* (a) and N_{dp} (b) (dash line: without temperature jump, and solid line: with temperature jump).

The results indicate that in the slip flow regime, *HTC* and N_{dp} with consideration of the effect of temperature jump have lower values compared to the case without this effect. This difference grows in the high values of *Kn* and *Nr*. This trend is analogous with the variation of these parameters in the continuum flow regime only for *Nr* = 50 and 100, while in other values of *Kn* and *Nr*, this behaviour is quite the reverse.

Fig. 8 describes the behaviour of *HTC* and N_{dp} regarding the changes in buoyancy parameter, *Ng* simultaneous with the variation of *Kn* in two cases with and without applying temperature jump condition. In the case of the non-existence of temperature jump condition, *HTC* increases with a rise in *Kn* in all values of *Ng*, especially *Ng* = 40 and 60. Note that in the boundary between the continuum and slip flow regimes, there is a turning point in the *HTC* variation. However, with consideration of temperature jump condition, *HTC* experiences a stable trend and approximately constant value along with the increase of *Kn* except for its high values in which *HTC* decreases. It is worth noting that without temperature jump condition and with the increase of *Ng*, the pressure drop has a downward trend from $Kn=10^{-4}$ to roughly $Kn=3\times10^{-4}$ following which N_{dp} rises, while in the case of applying the temperature jump condition, N_{dp} increases with growing *Ng* and also decreases with rising *Kn*. However, without temperature jump, N_{dp} sees the increasing growth in the continuum flow, especially in the high values of *Ng*, and then it gradually decreases in the slip flow except for *Ng*=40 and 60 in the high values of Kn.

Fig. 9 shows the changes in *HTC* and N_{dp} along with different heat flux ratios, ε, across a wide range of *Kn*. It is observable that *HTC* with the changes in heat flux ratio does not follow a particular trend, while N_{dp} decreases with increasing ε regardless of flow regime type. In continuum flow regime, the results of N_{dp} and *HTC* without considering temperature jump are lower than those with considering temperature jump, whereas this situation is opposite in slip flow regime. Moreover, it can be inferred from Fig. 9 that the highest and lowest values of heat transfer coefficient correspond to $\varepsilon = 0.5$ and $\varepsilon = 1$ respectively.

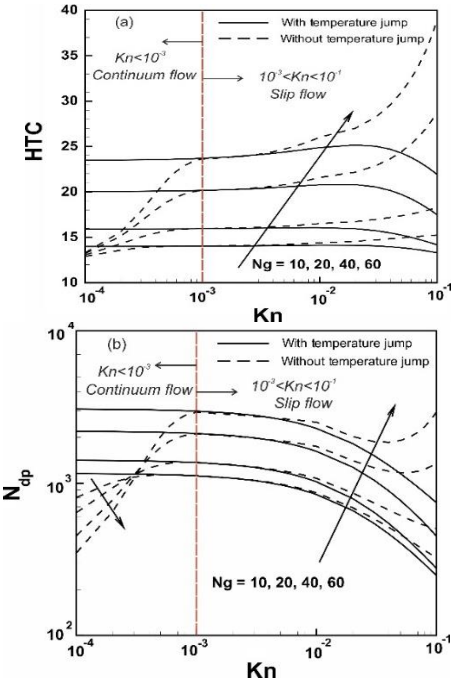

Fig. 8. Effect of temperature jump and *Ng* on *HTC* (a) and N_{dp} (b) (dash line: without temperature jump, and solid line: with temperature jump).

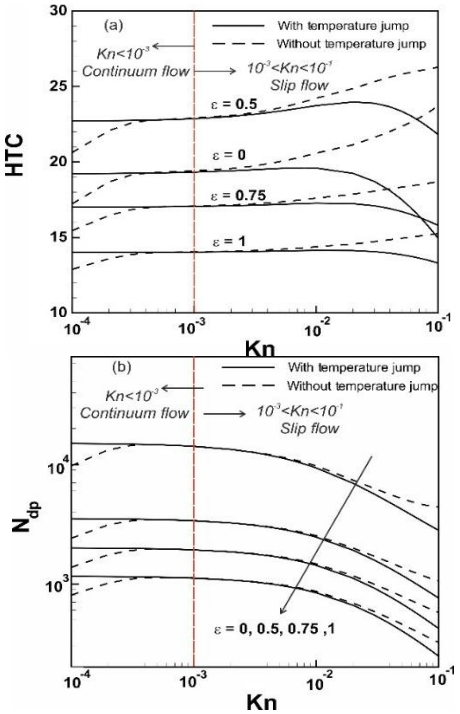

Fig. 9. Effect of temperature jump and ε on *HTC* (a) and N_{dp} (b) (dash line: without temperature jump, and solid line: with temperature jump).

8. Conclusions

In the present study, a proficient method for investigating nanofluid treatment has been implemented under circumstances of temperature jump and velocity slip near the boundaries. The main nanofluid flow features such as the velocity profile, temperature and nanoparticle volume fraction distributions were calculated by solving the equations as a set of ODEs along with proper boundary conditions in a vertical annulus. Additionally, the impacts of ϕ_B, *Nr*, *Ng*, and ε on *HTC* and N_{dp} in a broad range of *Kn* were obtained. All results have been computed in consideration of two cases of with and without temperature jump at walls in order to clarify the impact of temperature jump. Furthermore, the behaviour of *HTC* and N_{dp} has been studied with continuum and slip flow regimes. According to the obtained results in this paper, some highlighted points can be concluded:

1) Knudsen number is the parameter which directly influences velocity and temperature boundary conditions causing temperature jump and slip velocity near walls. Both these conditions are the controlling parameters on the temperature and nanoparticles concentration close to walls. However, applying temperature jump at walls causes the temperature profile to outstandingly vary, particularly in slip flow regime, while temperature jump negligibly influences the velocity profile and nanoparticles concentration.

2) Temperature jump at walls in slip flow regime causes *HTC* to have lower values than the case without this condition, irrespective of the variation of studied parameters. This behaviour is opposite in continuum flow regime, apart from the low values of *Nr*. So, the disregard of temperature jump near the walls in slip flow regime leads to the overvaluation of *HTC*, while in continuum flow regime this trend is reversed.

3) It can be concluded that in most cases, in the slip flow regime, considering the temperature jump at walls causes a decrease in N_{dp} compared to the case of consideration of without the temperature jump, however, in continuum flow regime, temperature jump leads to increasing the pressure drop.

References

[1] J. Maxwell, "Treatise on Magnetism and Electricity," *Vol II, Art*. pp. 717-9, (1873).

[2] S. U. Choi, J. A. Eastman, Enhancing thermal conductivity of fluids with nanoparticles. Argonne National Lab., IL (United States), (1995).

[3] H. Masuda, A. Ebata, and K. Teramae, "Alteration of thermal conductivity and viscosity of liquid by dispersing ultra-fine particles. Dispersion of Al2O3, SiO2 and TiO2 ultra-fine particles," *NETSU BUSSEI*. Vol. 7, No. 4, pp. 227-33, (1993).

[4] M. Sheikholeslami, "Influence of magnetic field on Al2O3-H2O nanofluid forced convection heat transfer in a porous lid driven cavity with hot sphere obstacle by means of LBM," *J. Mol. Liq.*, Vol. 263, pp. 472-88, (2018).

[5] M. Sheikholeslami, Z. Li, and A. Shafee, "Lorentz forces effect on NEPCM heat transfer during solidification in a porous energy storage system," *Int. J. Heat Mass Transfer*, Vol. 127, pp. 665-74, (2018).

[6] M. Sheikholeslami, "Finite element method for PCM solidification in existence of CuO nanoparticles," *J. Mol. Liq.*, Vol. 265, pp. 347-55, (2018).

[7] M. Sheikholeslami, M. Darzi, and Z. Li, "Experimental investigation for entropy generation and exergy loss of nano-refrigerant condensation process," *Int. J. Heat Mass Transfer*, Vol. 125, pp. 1087-95, (2018).

[8] M. Sheikholeslami, M. B. Gerdroodbary, S. V. Mousavi, D. Ganji, R. Moradi, "Heat transfer enhancement of ferrofluid inside an 90 elbow channel by non-uniform magnetic field," *J. Magn. Magn. Mater.*, Vol. 460, pp. 302-11, (2018).

[9] S. Jain, S. Bohra. *Hall current and radiation effects on unsteady MHD squeezing nanofluid flow in a rotating channel with lower stretching permeable wall*. Applications of Fluid Dynamics: Springer. (2018)

[10] S. Jain, R. Choudhary, "Combined effects of sunction/injection on MHD boundary

Layer flow of nanofluid over horizontal permeable cylinder with radiation," *J. Adv. Res. Dyn. Control Syst*., Vol. 11, pp. 88-98, (2017).

[11] A. Parmar, and S. Jain, "Influence of Non-Linear Chemical Reaction on MHD Convective Flow for Maxwell Fluid Over Three Different Permeable Vertical Surfaces," *J. Nanofluids*, Vol. 8, No. 4, pp. 671-82, (2019).

[12] M. Sheikholeslami, M. Jafaryar, S. Saleem, Z. Li, A. Shafee, and Y. Jiang, "Nanofluid heat transfer augmentation and exergy loss inside a pipe equipped with innovative turbulators," *Int. J. Heat Mass Transfer*, Vol. 126, pp. 156-63, (2018).

[13] M. Sheikholeslami, M. Jafaryar, and Z. Li, "Second law analysis for nanofluid turbulent flow inside a circular duct in presence of twisted tape turbulators," *J. Mol. Liq.* Vol. 263, pp. 489-500, (2018).

[14] M. Sheikholeslami, S. Shehzad, Z. Li, and A. Shafee, "Numerical modeling for alumina nanofluid magnetohydrodynamic convective heat transfer in a permeable medium using Darcy law," *Int. J. Heat Mass Transfer*, Vol. 127, pp. 614-22, (2018).

[15] M. Kerdarian, and E. Kianpour, "Flow field, heat transfer and entropy generation of nanofluid in a microchannel using the finite volume method," *J. Comput. Appl. Res. Mech. Eng.*, Vol. 8, No. 2, pp. 211-22, (2019).

[16] J. Buongiorno, "Convective transport in nanofluids," *J. Heat Transfer*, Vol. 128, No. 3, pp. 240-50, (2006).

[17] M. Sheikholeslami, "Numerical investigation of MHD nanofluid free convective heat transfer in a porous tilted enclosure," *Eng. Comput. (Swansea)*, Vol. 34, No. 6, pp. 1939-55, (2017).

[18] S. Moshizi, and I. Pop, "Conjugated effect of joule heating and magnetohydrodynamic on laminar convective heat transfer of nanofluids inside a concentric annulus in the presence of slip condition," *Int. J. Thermophys.*, Vol. 37, No. 7, pp. 72, (2016).

[19] T. Grosan, and I. Pop, "Fully developed mixed convection in a vertical channel filled by a nanofluid," *J. Heat Transfer*, Vol. 134, No. 8, pp. 082501, (2012).

[20] A. Aziz, W. Khan, and I. Pop, "Free convection boundary layer flow past a horizontal flat plate embedded in porous medium filled by nanofluid containing gyrotactic microorganisms," *Int. J. Therm. Sci.*, Vol. 56, pp. 48-57, (2012).

[21] M. Bahiraei, S. Mostafa Hosseinalipour, and M. Hangi, "Prediction of convective heat transfer of Al2O3-water nanofluid considering particle migration using neural network," *Eng. Comput. (Swansea)*, Vol. 31, No. 5, pp. 843-63, (2014).

[22] S. Moshizi, M. Zamani, S. Hosseini, and A. Malvandi, "Mixed convection of magnetohydrodynamic nanofluids inside microtubes at constant wall temperature," *J. Magn. Magn. Mater.*, Vol. 430, pp. 36-46, (2017).

[23] A. Malvandi, S. Moshizi, and D. Ganji, "Nanoparticle transport effect on magnetohydrodynamic mixed convection of electrically conductive nanofluids in micro-annuli with temperature-dependent thermophysical properties," *Physica E.*, Vol. 88, pp. 35-49, (2017).

[24] S. Moshizi, and A. Malvandi, "Magnetic field effects on nanoparticle migration at mixed convection of MHD nanofluids flow in microchannels with temperature-dependent thermophysical properties," *J. Taiwan Inst. Chem. Eng.*, Vol. 66, pp. 269-82, (2016).

[25] H. Xu, T. Fan, and I. Pop, "Analysis of mixed convection flow of a nanofluid in a vertical channel with the Buongiorno mathematical model," *Int. Commun. Heat Mass Transfer*, Vol. 44, pp. 15-22, (2013).

[26] C. Yang, W. Li, and A. Nakayama, "Convective heat transfer of nanofluids in a concentric annulus," *Int. J. Therm. Sci.*, Vol. 71, pp. 249-57, (2013).

[27] C. Yang, W. Li, Y. Sano, M. Mochizuki, and A. Nakayama, "On the anomalous convective heat transfer enhancement in nanofluids: a theoretical answer to the

nanofluids controversy," *J. Heat Transfer*, Vol. 135, No. 5, pp. 054504, (2013).

[28] D. Ganji, and A. Malvandi, "Natural convection of nanofluids inside a vertical enclosure in the presence of a uniform magnetic field," *Powder Technol.*, Vol. 263, pp. 50-57, (2014).

[29] A. Malvandi, and D. Ganji, "Effects of nanoparticle migration on force convection of alumina/water nanofluid in a cooled parallel-plate channel," *Adv. Powder Technol.*, Vol. 25, No. 4, pp. 1369-75, (2014).

[30] S. Moshizi, A. Malvandi, D. Ganji, and I. Pop, "A two-phase theoretical study of Al2O3–water nanofluid flow inside a concentric pipe with heat generation/absorption," *Int. J. Therm. Sci.*, Vol. 84, pp. 347-57, (2014).

[31] A. Malvandi, S. Moshizi, E. G. Soltani, and D. Ganji, "Modified Buongiorno's model for fully developed mixed convection flow of nanofluids in a vertical annular pipe," *Comput. Fluids*, Vol. 89, pp. 124-32, (2014).

[32] S. Kandlikar, S. Garimella, D. Li, S. Colin, M. R. King, *Heat transfer and fluid flow in minichannels and microchannels*: elsevier, (2005).

[33] A. Sohankar, M. Riahi, and E. Shirani, "Numerical investigation of heat transfer and pressure drop in a rotating U-shaped hydrophobic microchannel with slip flow and temperature jump boundary conditions," *Appl. Therm. Eng.*, Vol. 117, pp. 308-321, (2017).

[34] M. Smoluchowski von Smolan, "Ueber wärmeleitung in verdünnten gasen," *Ann. Phys. (Leipzig)*, Vol. 300, No. 1, pp. 101-30, (1898).

[35] M. Knudsen, "Die molekulare Wärmeleitung der Gase und der Akkommodationskoeffizient," *Ann. Phys. (Leipzig)*, Vol. 339, No. 4, pp. 593-656, (1911).

[36] A. Akbarinia, M. Abdolzadeh, and R. Laur, "Critical investigation of heat transfer enhancement using nanofluids in microchannels with slip and non-slip flow regimes," *Appl. Therm. Eng.*, Vol. 31, No. 4, pp. 556-65, (2011).

[37] C. Yang, Q. Wang, A. Nakayama, and T. Qiu, "Effect of temperature jump on forced convective transport of nanofluids in the continuum flow and slip flow regimes," *Chem. Eng. Sci.*, Vol. 137, pp. 730-739, (2015).

[38] H. Shokouhmand, A. M. Isfahani, and E. Shirani, "Friction and heat transfer coefficient in micro and nano channels filled with porous media for wide range of Knudsen number," *Int. Commun. Heat Mass Transfer*, Vol. 37, No. 7, pp. 890-894, (2010).

[39] J. Shalini, and S. BOHRA, "Soret/Dufour Effects on Radiative Free Convection Flow and Mass Transfer over a Sphere with Velocity Slip and Thermal Jump," *Walailak J. Sci. Tech.*,. Vol. 16, No. 9, pp. 701-721, (2019).

[40] A. Karimipour, "New correlation for Nusselt number of nanofluid with Ag/Al2O3/Cu nanoparticles in a microchannel considering slip velocity and temperature jump by using lattice Boltzmann method," *Int. J. Therm. Sci.*, Vol. 91, pp. 146-156, (2015).

[41] S. A. Sajadifar, A. Karimipour, and D. Toghraie, "Fluid flow and heat transfer of non-Newtonian nanofluid in a microtube considering slip velocity and temperature jump boundary conditions," *Eur. J. Mech. B/Fluids*, Vol. 61, pp. 25-32, (2017).

[42] M. Shojaeian, M. Yildiz, A. Koşar, "Heat transfer characteristics of plug flows with temperature-jump boundary conditions in parallel-plate channels and concentric annuli," *Int. J. Therm. Sci.*, Vol. 84, pp. 252-259, (2014).

[43] H. Brinkman, "The viscosity of concentrated suspensions and solutions," *J. Chem. Phys*., Vol. 20, No. 4, pp. 571-, (1952).

[44] B. C. Pak, and Y. I. Cho, "Hydrodynamic and heat transfer study of dispersed fluids with submicron metallic oxide particles," *Exp. Heat Transf.*, Vol. 11, No. 2, pp. 151-170, (1998).

[45] M. Gad-el-Hak, *MEMS: introduction and fundamentals*: CRC press, (2005).
[46] M. Hatami, M. Sheikholeslami, and D. Ganji, "Laminar flow and heat transfer of nanofluid between contracting and rotating disks by least square method," *Powder Technol.*, Vol. 253, pp. 769-79, (2014).
[47] N. A. Yacob, A. Ishak, I. Pop, and K. Vajravelu, "Boundary layer flow past a stretching/shrinking surface beneath an external uniform shear flow with a convective surface boundary condition in a nanofluid," *Nanoscale Res. Lett.*, Vol. 6, No. 1, pp. 314, (2011).
[48] T. Motsumi, and O. Makinde, "Effects of thermal radiation and viscous dissipation on boundary layer flow of nanofluids over a permeable moving flat plate," *Phys. Scr.*, Vol. 86, No. 4, pp. 045003, (2012).
[49] W. M. Kays, M. E. Crawford, B. Weigand, *Convective heat and mass transfer*: McGraw-Hill Higher Education Boston, (2005).
[50] W. Kays, M. Crawford, *Convective Heat and Mass Transfer*. New York: McGraw-Hill, (1980).

How to cite this paper:

Hamid Reza Ghaffarianjam, Sajad A. Moshizi, Mahdi Zamani and Mahdi Amiri Daluee, “Investigation of temperature jump and slip effects on nanofluid treatment inside a vertical annulus via modified Buongiorno’s model”, *J. Comput. Appl. Res. Mech. Eng.*, Vol. 10, No. 2, pp. 511-524, (2021).

DOI: 10.22061/jcarme.2019.5265.1653

URL: https://jcarme.sru.ac.ir/?_action=showPDF&article=1178